14 January 2000

ELSEVIER

Chemical Physics Letters 316 (2000) 191–198

CHEMICAL PHYSICS LETTERS

www.elsevier.nl/locate/cplett

The size distribution, imaging and obstructing properties of C_{60} and higher fullerenes formed within arc-grown single walled carbon nanotubes

Jeremy Sloan [a], Rafal E. Dunin-Borkowski [b], John L. Hutchison [b], Karl S. Coleman [a], V. Clifford Williams [a], John B. Claridge [a], Andrew P.E. York [a], Cigang Xu [a], Sam R. Bailey [a], Gareth Brown [a], Steffi Friedrichs [a], Malcolm L.H. Green [a,*]

[a] *Wolfson Catalysis Centre (Carbon Nanotechnology Group), Inorganic Chemistry Laboratory, University of Oxford, South Parks Road, Oxford, OX1 3QR, UK*

[b] *Department of Materials, University of Oxford, Parks Road, Oxford, OX1 3PH, UK*

Received 16 September 1999

Abstract

The relative size distributions of molecules of C_{60} and higher fullerenes observed in single walled carbon nanotubes (SWNTs) produced by arc vaporization of carbon in the presence of a mixed Ni/Y catalyst are described. The experimental and calculated imaging properties of the fullerenes, which were observed in ca. 5–10% of SWNTs, are also described. The in situ e-beam irradiation in a 300 kV field emission gun transmission electron microscope causes rapid coalescence of the fullerenes within the SWNTs. The incorporated fullerenes also directly impede crystal growth in SWNTs when their cavities are filled by the liquid phase capillary method. © 2000 Elsevier Science B.V. All rights reserved.

Keywords: C_{60}; Carbon; Crystallisation; FEGTEM; Fullerenes; Nanotubes; SWNTs; TEM

1. Introduction

Smith et al. have reported that chains of C_{60} molecules are present within single walled carbon nanotubes (SWNTs) formed by pulsed laser evaporation (PLV) of a catalyst-containing graphite target [1–3]. More recently, Zhang et al. observed fullerenes in as-prepared SWNTs formed by Ni/Y catalysed carbon arc evaporation [4]. These observations are significant as the presence of fullerenes in SWNTs formed by any method will influence the properties of the resultant carbon composites. For example, with respect to the filling of SWNTs with metals and metals halides [5–7], the presence of fullerenes could affect both the yield and homogeneity of halide/nanotube composites. Furthermore, any physical measurements obtained from SWNTs containing fullerenes must inevitably include some component from the incorporated molecules.

An important consideration with respect to the direct observation of fullerenes in SWNTs using

* Corresponding author. Tel.: +44-1865-272649; fax: +44-1865-272690; e-mail: malcolm.green@chem.ox.ac.uk

0009-2614/00/$ - see front matter © 2000 Elsevier Science B.V. All rights reserved.
PII: S0009-2614(99)01250-6

transmission electron microscopy (TEM) is their imaging behaviour. Smith et al. imaged chains of C_{60} molecules incorporated within SWNTs using a 400 kV TEM operated at 100 kV [1]. Their experimental images showed C_{60} molecules as well-defined 0.7 nm diameter black circles within the SWNTs, the outside walls of which appeared as parallel dark lines separated by 1.3–1.4 nm. The fullerene molecules were separated from the SWNT walls by a van der Waals gap of ca. 0.3 nm and were positioned along the SWNT capillaries at regular ca. 1.0 nm intervals. Given that these dimensions are within the resolution capabilities of most modern TEMs (typically 0.2–0.3 nm point resolution for a 200 kV TEM), it is perhaps surprising that the observation of C_{60} molecules in SWNTs was not made prior to late 1998 [1]. This may be due to the low yields of fullerenes incorporated in SWNTs or to the experimental conditions employed during their synthesis and subsequent processing (e.g., purification). Equally, however, the image contrast produced by C_{60} molecules incorporated in SWNTs within a particular TEM must be sufficient for them to be detected under the experimental conditions of observation.

Here we describe the formation, type and relative abundance of fullerenes produced in SWNTs by arc evaporation. We also address the imaging properties of these molecules when they are incorporated in SWNTs and describe their rapid coalescence when subjected to high electron flux in a 300 kV field emission gun transmission electron microscope (FEGTEM). Finally, we show how fullerene blockages in SWNTs inhibit crystal growth inside their capillaries when they are filled with liquid phase metal halides and speculate on a possible mechanism of formation for the encapsulated fullerenes.

2. Experimental

SWNTs were prepared using a high yield metal catalysed arc synthesis method similar to that reported by Journet et al. [3]. In a typical procedure, a 100 mm long 10 mm diameter graphite rod was machined down to a diameter of 6 mm with a 40 mm deep 3.5 mm diameter hole drilled along the central axis of the thin region. This cavity was packed with a mixture of 4.2 at% Ni and 1.0 at% Y mixed intimately with graphite powder. The composite rod was arc evaporated in a Krätschmer–Huffman soot box [8,9]. A heat shield (a 200 mm long, 100 mm diameter stainless steel cylinder) was placed around the electrodes to confine the carbon plasma. The evaporation was carried out in a dynamic vacuum with a 660 torr He, with a voltage of 25–30 V and a current of 110–140 A maintained between the electrodes. Nearly all of the SWNT samples that we describe were subjected to subsequent heat treatments during capillary filling experiments. The procedure for filling SWNTs by capillarity is described elsewhere [6,7].

The SWNT samples were examined at 300 kV in a JEOL JEM-3000F FEGTEM, which has a low spherical abberation coefficient (C_s) of 0.6 nm and a point resolution of between 0.16 and 0.17 nm [10]. Images were acquired digitally onto a Gatan model 794 (1 k × 1 k) CCD camera at an known objective lens current at which the magnification had been calibrated accurately using Si[110] lattice fringes. Image simulations were performed using a standard multi-slice algorithm that incorporated representative imaging parameters for a high-resolution image taken on the JEM-3000F (a focal spread of 8 nm, a beam semi-convergence of 0.6 mrad and an objective aperture of 0.1 nm) with nanotube and fullerene coordinates generated using algorithms developed by White et al. [11] and Yoshida and Osawa [12].

3. Results and discussion

Molecular fullerenes were found to be present inside between 5–10% of all of the observed SWNTs. In those SWNTs that contained fullerenes, they were almost always close-packed into continuous 'chains' and well-separated, discrete encapsulated molecules were rarely observed. Fig. 1a shows an example of a multiply filled bundle of SWNTs in which the three prominent tubules in the main bundle (more are present in projection) appear to be completely filled with close-packed fullerenes. One 'L'-shaped bent tubule visible on the left of the bundle is apparently empty. Fig. 1b–h show further examples of close-packed filled SWNTs, either in partially filled bundles (Fig. 1b, c and d), or discrete SWNTs (Fig. 1e,

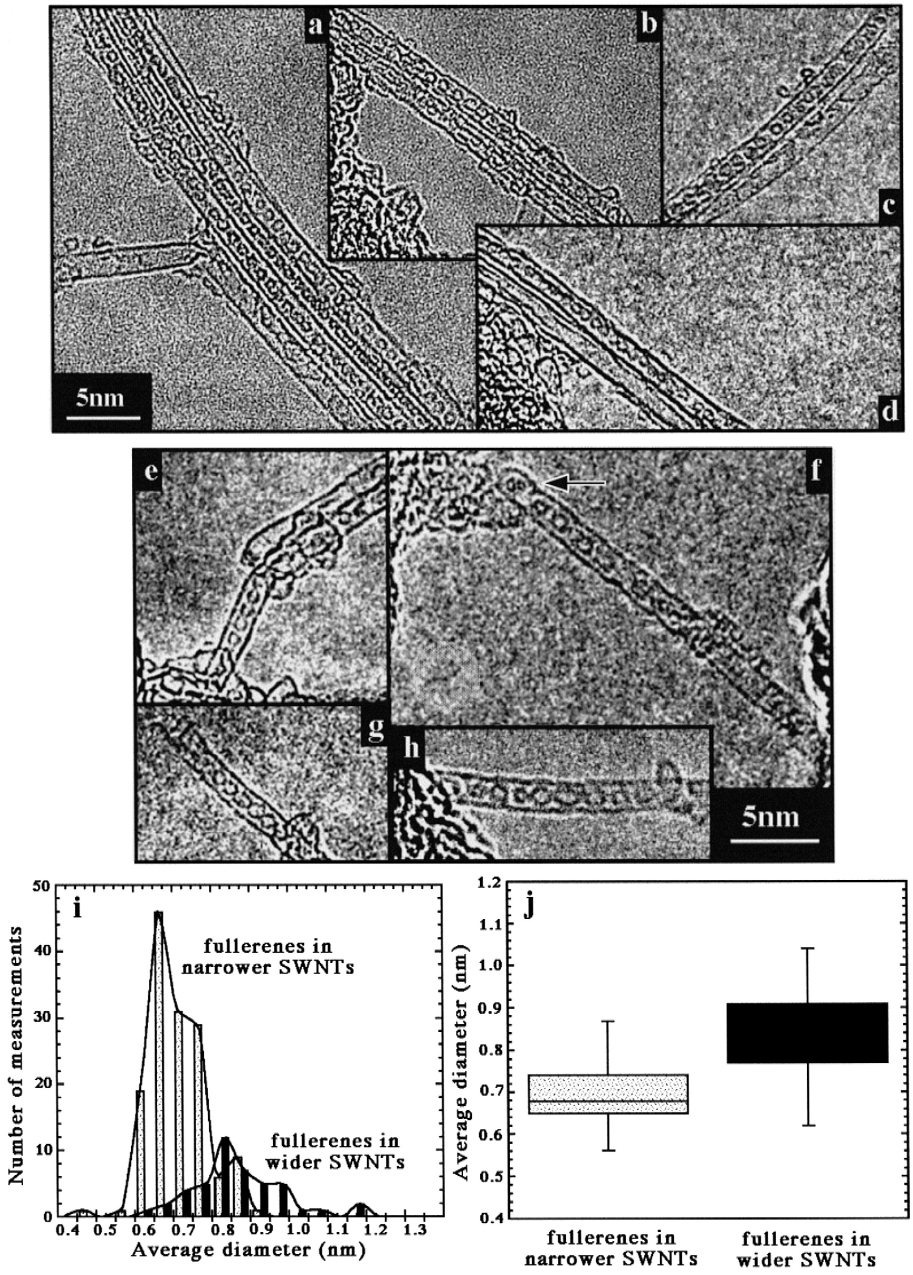

Fig. 1. Micrographs showing: (a) high density of fullerenes within a bundle of SWNTs; (b)–(d) Chains of fullerenes in partially occupied SWNTs; (e)–(f) Discrete filled SWNTs; (g) Discrete filled SWNT tip with small fullerenes at the tip (arrowed); (h) Discrete SWNT filled with fullerenes of variable diameter; (i) Measured fullerene diameters in SWNTs of 1.35–1.40 nm (light shading) and 1.55–1.60 nm (dark shading); (j) As for Fig. 1i but with boxes containing central 50% of measurements. The error bars indicate the overall spread in the data. The *x*-axis in this plot is arbitrary.

f, g and h). Most significantly, fullerenes with variable diameters were present inside SWNTs. While some fullerenes had diameters corresponding to that of C_{60} (ca. 0.7 nm), others were observed with

diameters in the range 0.8–1.1 nm, corresponding to the higher fullerenes (i.e., C_n with $n > 60$). A small number of fullerenes were also observed with diameters smaller than C_{60}, in the range 0.4–0.7 nm. The latter are unlikely to be 'elongated' fullerenes viewed in projection, as a result of the constricting nature of the SWNT capillary and, in particular, its van der Waals surface (see Fig. 2c, below). The smaller structures are more likely to correspond to lower fullerenes (i.e., C_n with $n < 60$) which, though not very common or stable, have been reported (e.g., C_{36} [13]).

Fig. 1i and j summarise our measurements with respect to the distributions of the diameters of encapsulated fullerenes in SWNTs. Separate graphs are plotted for fullerenes contained within SWNTs falling within two narrow diameter distributions of 1.35–1.40 nm and 1.55–1.60 nm. In Fig. 1j, the same data are plotted as bar graphs in which the central boxes contain the central 50% of the measured diameters while the error bars indicate the overall spread in the data. It is striking that both distributions in Fig. 1i are very similar in shape, with both exhibiting single dominant peaks coupled with prominent shoulders at larger diameters. The narrower nanotubes contain fullerenes with apparent diameters of between ca. 0.4 and 1.0 nm, while the wider nanotubes contain a broader size distribution of fullerenes that have diameters of between 0.6 and 1.1 nm. Diameters of 0.4–1.0 nm would correspond to $\sim C_{36}$–C_{90} fullerenes while diameters of 0.6–1.1 nm would correspond to $\sim C_{60}$–C_{120} fullerenes. Most importantly, the results show a clear correlation between nanotube diameter and encapsulated fullerene size, with a shift in the size distribution towards the larger fullerene diameters as the diameter of the SWNT increases. The estimated precision in the diameter measurements is ± 0.05 nm.

It is clearly difficult to know exactly which of the higher fullerenes (i.e., C_n with $n > 60$) are present within SWNTs merely from average diameters measured from TEM lattice images. This issue is further complicated by the fact that the higher fullerenes exhibit multiple isomeric forms with shapes ranging from approximately ellipsoidal ('rugby-ball') to spheroidal in nature [14]. More information can potentially be obtained about the structural properties of fullerenes incorporated within SWNTs by the careful comparison of image contrast obtained from experimental images and image contrast calculated from theoretical structural models by TEM image simulation [15,16].

The first column in Fig. 2a shows a sequence of four experimental through-focal images obtained from a discrete SWNT containing a chain of 14 fullerenes of approximately equal diameter. It is only close to Scherzer defocus (second image from top), that the fullerenes image as distinct black circles ca. 0.8 nm in diameter. The middle left column shows the image contrast simulated to scale for a chain of a string of C_{60} molecules incorporated within a (10,10) SWNT for $+70$ nm (overfocus), -50 nm (Scherzer defocus), -80 nm (underfocus) and -140 nm (underfocus) focal values, respectively. The middle right column shows the same simulated images but with added noise in order to mimic the experimental conditions. While the series of simulated images reproduce approximately the image contrast of the experimental images, the calculated contrast of the incorporated C_{60}s – particularly at Scherzer defocus – do not match well with the experimental images. A much better match is obtained for a sequence of images calculated for the same focal values from a model corresponding to a chain of C_{80} molecules incorporated within an (11,11) SWNT, as shown in the right hand column of Fig. 2a. The structural model and corresponding projected potential diagram are plotted in Fig. 2b. A van der Waals surface diagram for the second case is shown in Fig. 2c. The latter shows how the C_{80} molecule can only just be accommodated by the (11,11) tubule.

An extended calculated through focal series of images (not shown) showed that the focusing range for which both types of fullerenes are clearly visible exists only over a very narrow focal range between about -30 to -60 nm defocus for our instrument. In Fig. 2d, the percentage contrast the wall of a simulated (10,10) SWNT (solid line) and that of the wall of a C_{60} molecule (dotted line) are plotted as a function of the defocus. Note that the contrast of the SWNT wall and that of the C_{60} molecule are only equal at ca. -47 nm defocus (i.e., Scherzer defocus) and -20 nm defocus. In Fig. 2e, a bar graph showing the measured experimental contrast following correction for the point spread function of the CCD camera is shown, with the dark columns showing the

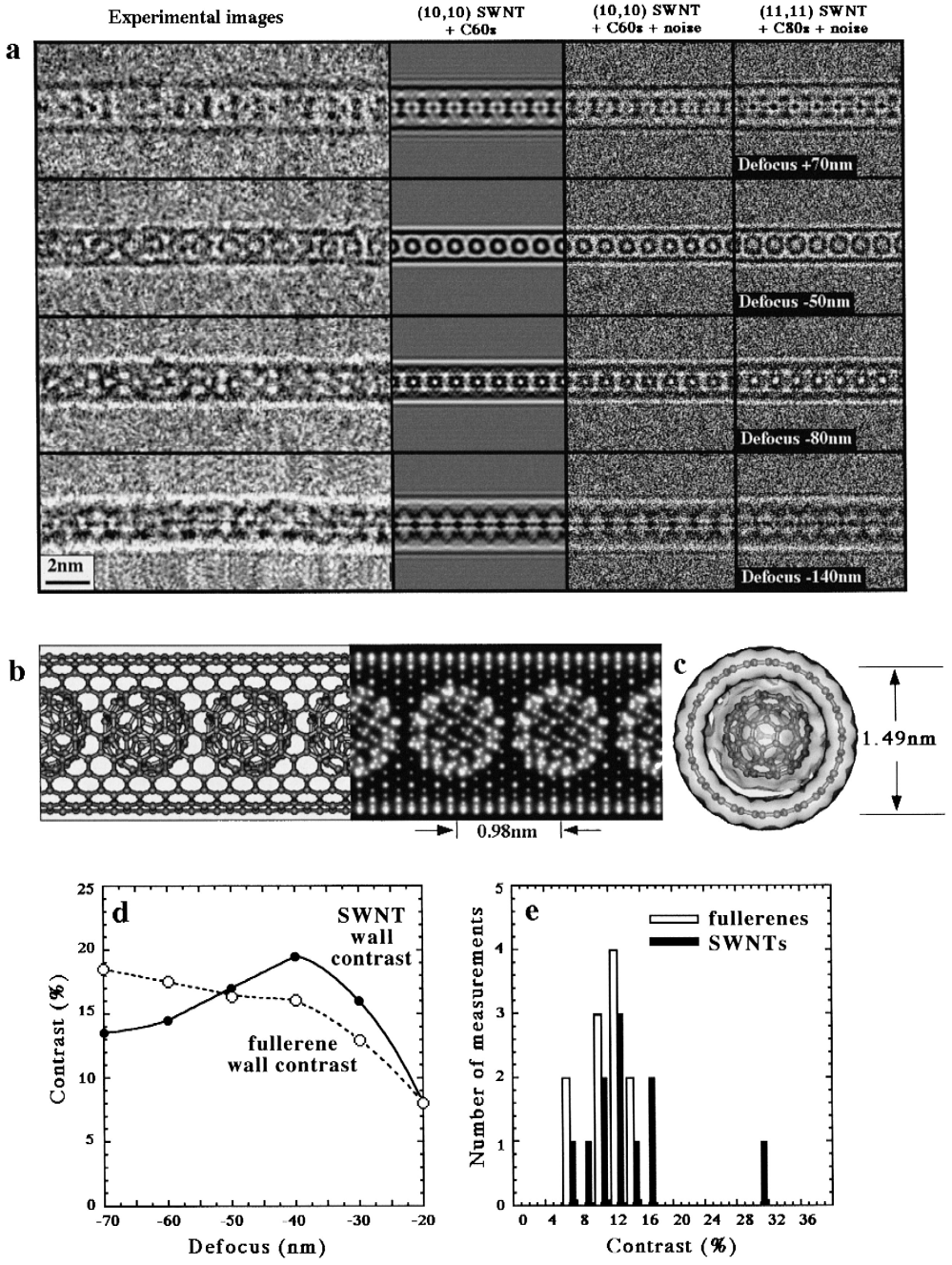

Fig. 2. (a) Experimental through focal series of a SWNT filled with fourteen fullerene molecules (left column). The middle left column shows image simulations calculated for a chain of C_{60} molecules in a (10,10) SWNT and the middle right column shows the same simulations with added noise. The right column shows image simulations with added noise calculated for a (11,11) SWNT incorporating a chain of C_{80} molecules; (b) Structural representation (left) and computed projected potential (right) for the C_{80}/SWNT composite; (c) 'End-on' structural representation showing the van der Waals surface for a C_{80} inside a (11,11) SWNT; (d) and (e) Plots showing the relationship between contrast and defocus from simulated and experimental images, respectively.

measurements for the SWNT walls and the light columns showing the corresponding measurements for the fullerene walls. Although the simulations were performed for representative rather than measured experimental parameters, it is satisfying that the experimental and simulated contrast are found to be almost identical on an absolute scale.

The encapsulated fullerenes were observed to both rearrange and coalesce following exposure to high electron flux in the FEGTEM, two examples of which are shown in Fig. 3a and b. Following irradiation at 300 kV for a period of ca. 5 min, the initially discrete fullerenes (Fig. 3a, top micrograph) coalesce first to produce dimers and then trimers within the SWNT capillary (middle micrograph). Eventually the fullerenes then form a continuous secondary (ca. (5,5)) nanotube within the encapsulating SWNT. The second sequence of images in Fig. 3b shows coalescence and fullerene rearrangement occurring over a slightly shorter time scale (ca. 3 min). Similar phenomena were noted by Smith et al. for fullerenes exposed to a 100 kV electron beam [1]. The beam current density used in our experiments was approximately 5×10^5 $e^-/nm^2/s$ which corresponds to $\sim 2 \times 10^5$ electrons passing through a C_{60} molecule every second, equivalent to a current of 3×10^{-14} A.

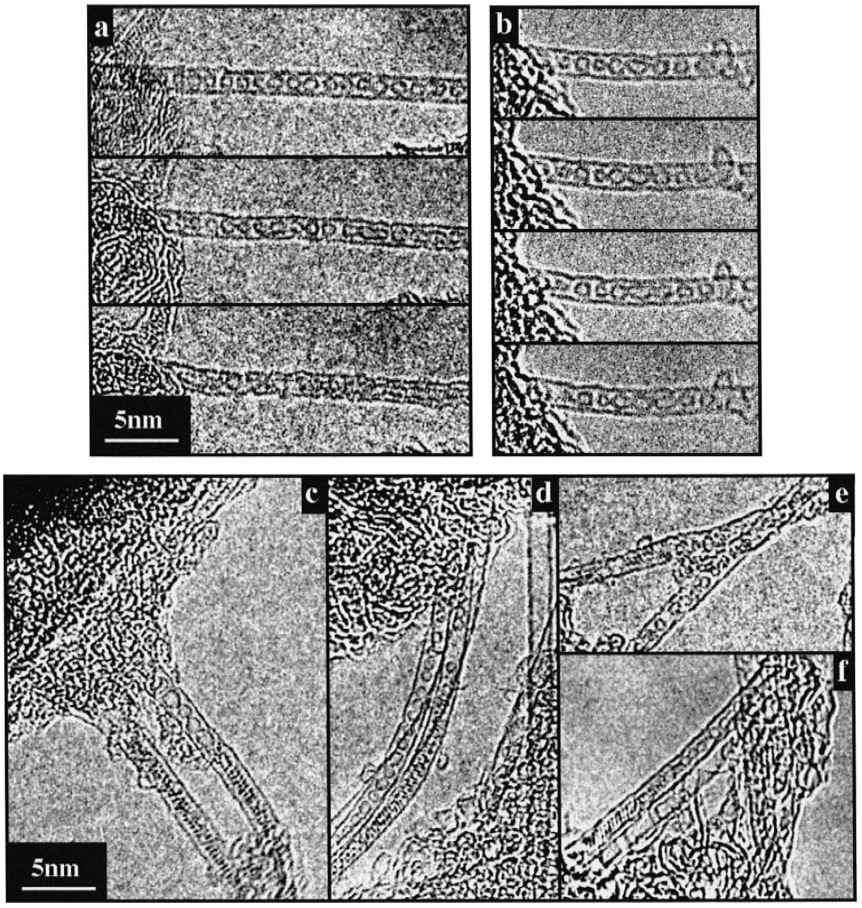

Fig. 3. (a) Sequence of images showing the coalescence of fullerene molecules within a discrete SWNT over ca. five minutes. Discrete fullerenes (top image) coalesce to form dimers and trimers (middle image) which eventually coalesce completely to form a (5,5) SWNT within the capillary (bottom image); (b) Second series of micrographs showing fullerene coalescence obtained over ca. two minutes; (c) (d–f) Micrographs showing blockage of SWNT capillaries by C_{60} molecules when filled with a mixture of KCl-$ThCl_4$, CsCl and $CdCl_2$ (two examples), respectively.

One important consequence of the presence of fullerenes inside SWNTs concerns the incorporation of foreign materials within SWNTs [5–7,17]. In this laboratory, the filling of SWNTs via capillary filling, either from solution [5] or by capillary wetting with either pure phases or mixtures of metal halides, has been achieved [6,7]. Several examples of 'blockages' of the SWNT capillaries with fullerenes leading to the restriction of crystal growth within them, are shown in Fig. 3c–f. In Fig. 3c, two discrete SWNTs filled with a mixture of $ThCl_4$ and KCl are shown. The $ThCl_8$ polyhedra are visible as intense dark spots within the SWNT capillaries. Crystal growth within one of the SWNTs is clearly restricted by a blockage consisting of four fullerenes with diameters of 0.7–1.0 nm. Related examples are shown for CsCl (Fig. 3d) and $CdCl_2$ (Fig. 3e and f).

Prior to the preliminary observations of fullerenes in SWNTs, Rinzler et al. showed by Raman spectroscopy that C_{60} is present as an adduct in acid purified PLV prepared SWNTs while Birkett et al. have suggested that C60 and higher fullerene molecules, together with atomistic Ni, template the formation of SWNTs during growth [2,18]. Smith et al. have suggested that these molecules self-assemble within SWNTs [1]. Zhang et al., however, have also noted the formation of molecular fullerenes within as-produced SWNTs prepared by the arc evaporation method [4], an observation reinforced by the results in Fig. 3c–f which suggest that fullerene molecules are 'trapped' within the SWNTs by the filling media. Given that the temperature of formation of SWNTs by both the PLV and arc evaporation techniques are in the same range, it is unlikely that the mode of formation of fullerenes within SWNTs is substantially different in either case.

We offer the following speculative mechanism for fullerene incorporation within SWNTs. The formation of empty SWNTs proceeds by carbon vapour diffusion into a nickel particle and a SWNT grows and propagates from one face of the Ni particle (Fig. 4a). In the case of SWNT/fullerene formation, a smaller diameter incipient SWNT grows from the Ni surface and inside the larger encapsulating SWNT (Fig. 4b). However, possibly due to the stabilising effect of the outer SWNT, the incipient inner SWNT 'pinches off' giving rise to discrete fullerenes inside the outer SWNT (Fig. 4c). The fullerene molecules have enough residual thermal energy, either from condensation from the hot arc environment or supplied during subsequent heat treatments (e.g., as from capillary filling experiments), to move around inside the SWNT capillaries and then form contiguous fullerene 'chains' in the SWNT capillaries (Fig. 4d).

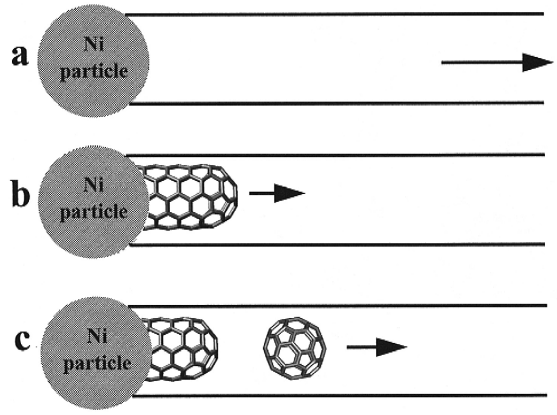

Fig. 4. Schematic diagrams showing: (a) Propagation of 'empty' SWNT from a Ni particle or face; (b) Propagation of a SWNT and a smaller incipient SWNT within the larger nanotube capillary; (c) 'Pinching off' of a C_{60} fullerene from incipient SWNT.

4. Conclusions

We have observed significant quantities of fullerenes spanning the range C_{36}–C_{120} incorporated within SWNTs of different diameters formed by the catalytically assisted arc evaporation technique. The TEM imaging properties of the encapsulated fullerenes have also been investigated. Fullerene formation within SWNTs has been observed to impede crystal growth within SWNTs, and a mechanism for fullerene formation within SWNTs has been proposed.

Acknowledgements

We wish to acknowledge the Petroleum Research Fund, administered by the American Chemical Society (Grant No. 33765-AC5), the EPSRC (Grant Nos. GR/L59238 and GR/L22324) and Colebrand for

financial support. We also thank Adam Palser and David E. Manolopolos, of The Physical and Theoretical Chemistry Laboratory, Oxford, for supplying the routine used to calculate nanotube coordinates.

References

[1] B.W. Smith, M. Monthoux, D.E. Luzzi, Nature 396 (1998) 323.
[2] A.G. Rinzler, A.G. Rinzler, J. Liu, H. Dai, P. Nikolaev, C.B. Huffman, F.J. Rodriguez-Macias, P.J. Boul, A.H. Lu, D. Heymann, D.T. Colbert, R.S. Lee, J.E. Fischer, A.M. Rao, P.C. Eklund, R.E. Smalley, Appl. Phys. A 67 (1998) 29.
[3] C. Journet, W.K. Maser, P. Bernier, A. Loiseau, M. Lamy, M.L. de la Chappelle, S. Lefrant, P. Derniard, R. Lee, J.E. Fischer, Nature 388 (1997) 756.
[4] Y. Zhang, S. Iijima, Z. Shi, Z. Gu, Phil. Mag. Lett. 79 (1999) 473.
[5] J. Sloan, J. Hammer, M. Zweifka-Sibley, M.L.H. Green, Chem. Commun. (1998) 347.
[6] J. Sloan, D.M. Wright, H.G. Woo, S. Bailey, G. Brown, A.P.E. York, K.S. Coleman, J.L. Hutchison, M.L.H. Green, Chem. Commun., (1999) 699.
[7] J. Sloan, S. Bailey, G. Brown, K.S. Coleman, R.E. Dunin-Borkowski, D.M. Wright, H.-G. Woo, J.B. Claridge, A.P.E. York, C. Xu, V.C. Williams, S. Friedrichs, R.L. Callender, J.L. Hutchison, M.L.H. Green, in preparation.
[8] W. Krätschmer, L.D. Lamb, K. Fostiropoulos, D.R. Huffman, Nature 347 (1990) 354.
[9] T.W. Ebbesen, P.M. Ajayan, Nature 358 (1992) 220.
[10] J.L. Hutchison, R.C. Doole, R.E. Dunin-Borkowski, J. Sloan, M.L.H. Green, JEOL News 34E (1999) 10.
[11] C.T. White, D.H. Robertson, J.W. Mintmire, Phys. Rev. B 47 (1993) 5485.
[12] M. Yoshida, E. Osawa, Bull. Chem. Soc. Jap. 68 (1995) 2073.
[13] C. Piskoti, J. Yarger, A. Zettl, Nature 393 (1998) 771.
[14] M.S. Dresselhaus, G. Dresselhaus, P.C. Eklund, The Science of Fullerenes and Carbon Nanotubes, Academic Press, London, 1995.
[15] J.M. Cowley, A.F. Moodie, Acta Cryst. 10 (1957) 609.
[16] J.M. Cowley, A.F. Moodie, Acta Cryst. 12 (1959) 353.
[17] L. Grigorian, K.A. Williams, S. Fang, G.U. Sumanasekera, A.L. Loper, E.C. Dickey, S.J. Pennycook, P.C. Eklund, Phys. Rev. Lett. 80 (1998) 5560.
[18] P.R. Birkett, A.K. Cheetham, B.R. Eggen, J.P. Hare, H.W. Kroto, D.R.M. Walton, Chem. Phys. Lett. 281 (1997) 111.